Future Augmented Reality in Endosurgery

Bojan Nokovic
Mariner Endosurgery
Hamilton, Canada
Email: bnokovic@marinerendosurgery.com

Tian Zhang
Mariner Endosurgery
Hamilton, Canada
Email: tzhang@marinerendosurgery.com

***Abstract*—We present technology that uses a computer-generated 3-D image inserted in real-time endoscopic view. The generated image represents the safe zone, the area in which the tip of the surgical tool should stay during operation. Movements of tools can be tracked using existing techniques of surgical tools navigation based on tracking fiduciary markers. We describe a spatial measurement system and explain the process of virtual zone creation, challenges related to the accuracy of the augmented reality system and calibration process that can be improved by machine learning techniques. We discuss possible future usage of this system in telesurgery both on the ground and in space.**

***Keywords*—Augmented reality; image processing; endosurgery**

I. Introduction

Augmented reality (AR) is a real-time view of physical world combined with computer-generated images creating a mixed reality (MR). The amount of information in AR is always greater than in reality itself. AR enhances the user's perception of and interaction with the real world. By using the latest AR techniques and technologies, the information about the surrounding real world becomes interactive and digitally usable [1]. The human perceptual system is highly tuned to space-time relationships. Dr. F. Brooks was the first to point out that visualization is *intelligence amplification* [2]. AR visualization goes step further; by increasing our understanding and interpretation of reality, it pushes our mental impression to an even higher level, creating *intelligence amplification*++.

We assume that AR is not restricted to a head-mount display (HMD), but can be any display that in real-time shows information.

Endosurgery is a medical field that practices minimally invasive internal surgery (MIS) that uses the endoscope to look inside the body [3]. Laparoscopic surgery, also referred to as keyhole surgery, is a surgical technique in which operations are performed through small incisions (usually 0.5-1.5 cm). The main advantage of laparoscopic vs. open surgery is that because of smaller incisions recovery time is shorter, and pain is reduced. The procedure is observed by the endoscopic digital camera that in real-time projects an internal view of the body to the surgical display.

These advantages are achieved, however, only if the procedure is performed completely without effective errors. Unfortunately, such errors are not uncommon in laparoscopic surgeries. Indeed, intra-operative and post-operative complications are prevalent with laparoscopic surgery procedures. Because of this, there is a need to improve patient safety during laparoscopic surgery so that the benefits derived from such procedures are achieved while the drawbacks are reduced or eliminated. One of the most profound drawbacks of laparoscopic surgery is the occurrence of unintentional or inadvertent injuries to patient tissue structures adjacent to, or sometimes distant from the intended surgical site or field. In the pelvic cavity, for example, bowels, ureters, large organs and blood vessels can be injured either directly from the heat or sharpness of the laparoscopic instruments, or burned indirectly through the conduction of heat through nearby tissues. Typically, such injuries are not appreciated at the time of surgery because the specific injury sites are hidden by blood or other patient tissues. Another disadvantage relevant to such iatrogenic injuries, is that the response to the unintended injury manifested by the patient is often a delayed one. This delayed response can be traumatic as well as tragic, and can sometimes result in one or more further surgeries, which would otherwise be unnecessary [4].

The AR can be used to indicate a *safe* or *unsafe* zone and to warn the surgeon in real-time if the surgical tool is approaching safe zone boundary. The image of the safe zone that is generated by a computer can be combined with camera image in real-time. In addition to this, image processing may indicate a rapid change in image contentment, like bleeding, blister, etc.

Areas of current AR implementation are education, medical, advertising, entertainment, mobile applications for smartphones, etc. [1]. In this paper, we are focused on AR in medical, surgical procedures and possible usage of this technology not only on surgical procedures on Earth but also for future telesurgical modus operandi in space.

A key challenge when developing AR systems in surgery is to verify that the accuracy of the position of computer-generated images in the live video stream meets system specification. In addition to technical challenges, other issues regarding to AR deployment in endoscopic surgery are related to education and retraining of the medical staff, but those are out of the scope of this paper.

In Section II we briefly describe related works. In Section III we describe spatial measurement system, calibration methodologies, and accuracy of measurement. In Section IV we describe the innovative process of virtual zone creation and image overlay technique in laparoscopic surgery. In Sections V, VI we represent the future usage of this technology in telemedicine robotics, especially in future space telesurgery [5]. In Section VII we look at regulations and possible approval of virtual zone in endosurgery.

II. Related Works

Significant research has been made to incorporate AR with medical imaging [6]. Video images of the operating site inside the body are recorded by an endoscopic camera device and presented on the surgical monitor is one example. However, displayed image and position of surgical tools are viewed in 2-D. That limitation can be partially eliminated by navigation surgical tools and techniques that augment the physician's view [6].

Italian research group ICAR CNR [7] works on many projects related to the visual presentation of noninvasive imaging on advanced multi-function display. The goal is to develop software technologies and novel methodologies for morphological and functional medical imaging applications.

The AR can be used to manage patient's medical history for post-stroke rehabilitation, treatment of psychological disorders, augmented navigation of visually impaired, etc. [1]. For instance, the doctor can check a patient's medical record by donning a head-mounted display (HMD) and looking over the patient to see virtual labels showing the patient's past injuries and illnesses [1]. So far HMD is used for 3-D visualization, HMD is tracked to compute an appropriate perspective and tested to increase the clinical acceptance of augmented reality. However, HMD systems still have a problem of lag for motion parallax and cannot provide a natural view for multiple observers [8].

Visual tracking in minimally invasive surgery that uses image processing of surgical tools with special markers is presented in [9]. The main idea is that the surgeon can use a gesture such as opening and closing the laparoscopic instrument (e.g. grasper). This gesture is recognized by advanced image processing system as the command to overlay a previously taken computed tomography (CT) or magnetic resonance imaging (MRI) pictures to the endoscopic camera view.

Ultrasound augmented with virtual reality for intracardiac surgery is presented in [10]. Tracking is provided by Aurora magnetic tracking system that determines a spatial position (sub-millimetric) and orientation (sub-degree) tracking. They clearly showed that limitation of ultrasound tracking (absence of direct vision) could be corrected by overlaying AR on tracked 2-D or 3-D ultrasound image.

III. Spatial Measurement System

The combination of spatial measurement systems that can position system in 3-D and medical images, know as image-guided surgery (IGS), was introduced in the 1990s [11]. Typically, a set of fiducial markers is secured to the surgical instrument.

Fig. 1. Passive NDI polaris tool.

All aspects of the design, construction, and characterization of tools used with NDI Polaris Systems [12] are described in [13]. NDI is the producer of highly precise and robust 3-D measurement tracking devices. The optical measurement system measures the 3-D positions of spherical markers. The position of the spherical markers determines the position of the surgical tools. Markers are used to track the tool during IGS. The process of IGS combines spatial measurement with medical imaging, typically CT or MRI. In standard IGS procedure, images are registered with the patient's position, and AR visualization of such structures is provided to the surgeon [14].

A. Zone

The condition that must be satisfied during a surgical procedure can be represented as the 3-D structure called the *safe zone*, an area in which surgical tools must be localized during the operation process. The safe zone can be created by the surgeon or by surgical robot assistant, [15] by a tool similar to the one shown in Fig. 1. The area arbitrarily close to the safe zone boundary is called the *critical zone*, it is 2-3 mm inside the safe zone. The area outside of safe zone boundary (even if it is in camera view) is considered to be the *unsafe zone*.

B. Tracking

Fig. 2. Laparoscopic scissors with passive markers.

By attaching a rigid body containing passive markers to laparoscopic scissors, as shown in Fig. 2, it is possible to track and record the 3-D position of the tip of the scissors in real-time during laparoscopic surgery operation. If during the procedure the tip of the tool exits the safe zone, a warning will be generated.

TABLE I. NDI TOOL ACCURACY [MM]

NDI 8700340			
Test #	3-D RMS Error	Mean Err.	Max 3-D Err.
1	0.32	0.29	0.56
2	0.39	0.35	0.80
3	0.40	0.36	0.84

TABLE II. SCISSORS WITH NDI RIGID BODY ACCURACY [MM]

Surgical Scissors with NDI RB			
Test #	3-D RMS Error	Mean Err.	Max 3-D Err.
1	0.54	0.47	1.48
2	0.53	0.47	1.39
3	0.52	0.47	1.30

C. Safe Zone Registration

Image registration is the process of overlaying images of the same scene taken from different viewpoints [16]. Registration brings images into geometric alignments.

D. Accuracy

International Standard Organization (ISO) defines accuracy as the combination of *trueness* and *precision* [17], [18]. Trueness is the difference between measured and true position. Precision is a measure of repeatability.

The accuracy of spatial measurement systems is usually given as root-mean-square (RMS) distance error [11]. The positions measured by measurement system $\vec{r}_m$ are compared to reference position acquired by a coordinate measuring machine (CMM) $\vec{r}_r$ on a point by point basis. The RMS determined over the volume of N points is given by:

$$\sqrt{\frac{1}{N}\sum_{i=1}^{N}(\vec{r}_{r_i} - \vec{r}_{m_i})^2} \tag{1}$$

The overall volume RMS for NDI Polaris system is less than 0.35 mm for a single marker. We tested the rigid body shown in Fig. 1; the result is shown in Table I.

In next experiment, we tested the accuracy of the rigid body attached to the surgical tool shown in Fig. 2. The result is in Table II.

In both cases, the origin is at the probe tips. From the chart shown in Fig. 3, which is taken from [11] it is evident that accuracy for longer laparoscopic surgical tools is lower than for shorter tools.

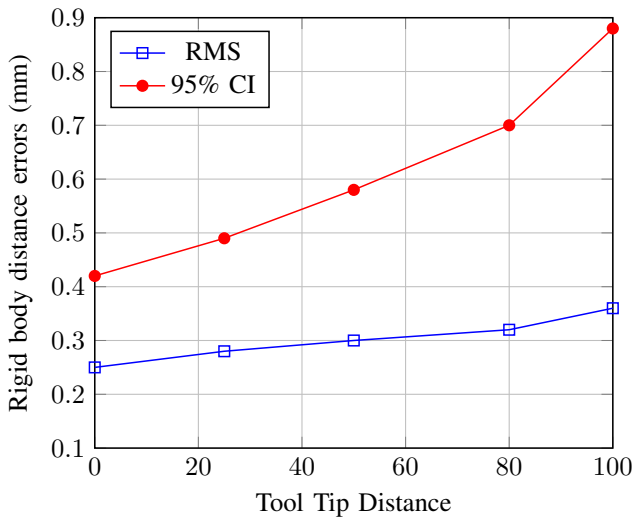

Fig. 3. Error vs. tool length [11].

E. Calibration by Block Calibrator

To estimate tool tip offset of the surgical tool, we need to attach an NDI body and place the tool into the calibrator as shown in Fig. 4. Ideally, the tip of a surgical tool must lie exactly at the origin of the calibrator rigid body geometry. Now, the infrared camera will report the data from NDI rigid body attached to scissors and the data from the calibrator rigid body.

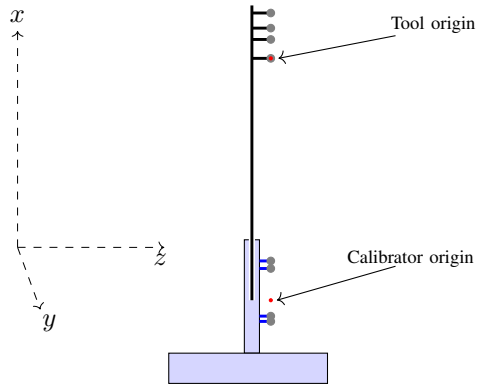

Fig. 4. Calibrator with inserted tool.

The difference between the tool origin (x_t, y_t, z_t) and calibrator origin (x_c, y_c, z_c) is offset Δz, shown in Fig. 5. The calibrator origin is closer to the IR tracker (camera).

F. Calibration by Pivoting

Pivoting is the process of moving tool 45 degrees forward-backward, and 45 degrees left-right from the initial straight position.

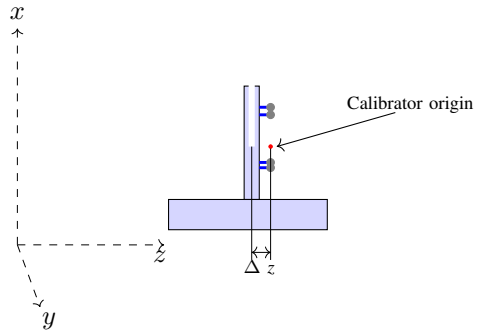

Fig. 5. Calibrator sphere offset.

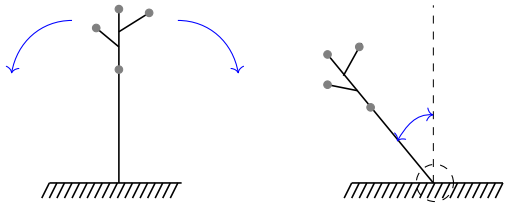

Fig. 6. Tool pivoting left-right and forward-backward.

The IR camera collects the position of the rigid tool body and reports its origin at a rate of up to 60 frames per second. The tool has to be moved from initial position to 45 degrees forward, backward 90 degrees and back to the original position. The movement must be completed in 10 sec. A similar movement is repeated going left-right-left. During this process that lasts 20 sec., the camera reports about 1200 positions that are distributed on the spherical surface; the centre of the sphere is the pivoting point. We can use method similar to one described by W.H. Beyer [19] to find the center and radius of the sphere:

$$(x_t - x_c)^2 + (y_t - y_c)^2 + (z_t - z_c)^2 = R.$$

(x_t, y_t, z_t) is the reported origin of the tool, and (x_p, y_p, z_p) position of the pivoting point. We need at least four origin tool positions to determine the pivoting point or center of the sphere. For instance for reported positions (3,2,1), (1,-2,-3), (2,1,3), (-1,1,2)

$$\begin{vmatrix} x_t^2 + y_t^2 + z_t^2 & x_t & y_t & z_t & 1 \\ 3^2 + 2^2 + 1^2 & 3 & 2 & 1 & 1 \\ 1^2 + (-2)^2 + (-3)^2 & 1 & -2 & -3 & 1 \\ 2^2 + 1^2 + 3^2 & 2 & 1 & 3 & 1 \\ (-1)^2 + 1^2 + 2^2 & -1 & 1 & 2 & 1 \end{vmatrix} = 0$$

Solving upper determinant we get

$$x^2 + y^2 + z^2 - \frac{48}{19}x + \frac{32}{19}y - \frac{8}{19}z = 0$$

$$(x - \frac{24}{19})^2 + (y - \frac{16}{19})^2 + (z - \frac{4}{19})^2 = \frac{4230}{361}$$

so the centre of the sphere is at

$$x_c = \frac{24}{19} \quad y_c = \frac{16}{19} \quad z_c = \frac{4}{19}$$

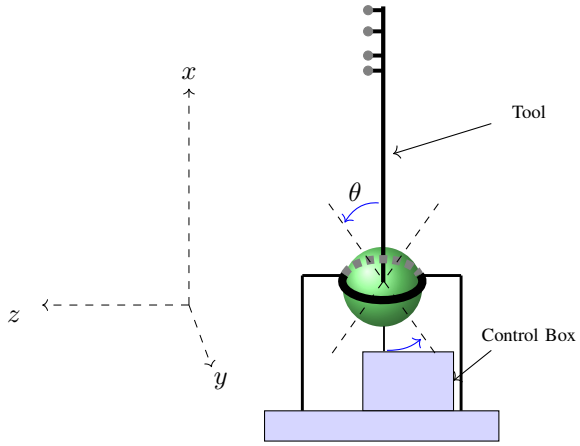

Fig. 7. Pivoting technique, tool tip in the centre of the ball.

If tool tip is sharp, the pivoting technique on the flat surface shown in Fig. 6 and on the ball shown in Fig. 7 have proximately the same accuracy. But in general when the tip of the tool is not sharp, pivoting on the ball is more accurate. During pivoting process about 1200 3-D positions are collected. We can calculate

$$\binom{1200}{4} = \frac{1200!}{4!(1200-4)!} \approx 86\ billion$$

centres of the sphere. Such calibration would be time consuming. Given that the calibration has to be done in 2-3 min, we need to extract the combination of points that gives us the most accurate estimation. Those are points that have the longest distance, taking into account that error in z-plane is greater than in x and y [20]. This is a typical problem that can be solved by *classification* that is a core component of machine learning. When the set of ten combinations of four points is selected, the centre of the sphere is calculated for each of the ten combinations. The calibrated value is the RMS of the ten calculated approximations according to (1).

G. Tracking Accuracy

High spatial measurement system accuracy is crucial for image-guided surgery. But accuracy assessment for systems tracking rigid bodies are ambiguous, and accuracy depends on many factors, like the number of markers, position of the markers to the camera, and external interference. *The cornerstone requirement for any measurement system remains whether its accuracy is sufficient for the intended application* [11].

The general approach in accuracy analysis of a geometrical structure with fiducial markers registration accommodates *Fiducial Localization Error* (FLE), the distance between a measured position and true position of a single marker. FLE can be varying from point to point (inhomogeneous) and with the direction (anisotropic) [21].

For the systems with several markers accuracy is described by *Fiducial Registration Error* (FRE), that is the positioning error of a rigid body (system with markers) after registration. *Target Registration Error* (TRE) is the positioning error of any point of a tool excluding markers, most commonly the tool tip [17], as shown in Fig. 3.

H. Overall System Accuracy

Image overlay error is about (3.5 mm $\pm$ 1.5 mm), but system accuracy is determined only by tool tracking precision. Tracking inside 3-D virtual zone has an RMS accuracy of 2.5 mm.

I. Interference

The charge-coupled devices (CCDs) on the IR tracker are sensitive only to light in range 800 nm to 1.1mm (frequency range between 375 THz and 272 GHz) shown in Fig. 8 [22].

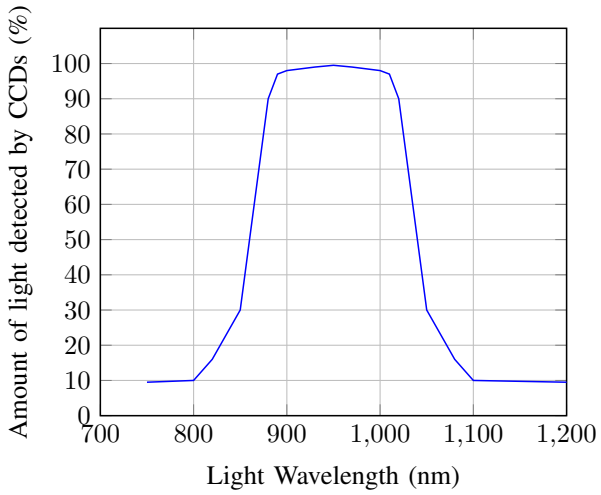

Fig. 8. Filter spectral response.

If environmental light has a strong IR component, it may interfere to the system. Although some operating room lights may emit IR, typical surgical LED light spectra given at Fig. 9 has reduced the IR component. Further reduction, if needed, is possible by special filters that can reduce IR component by more than ten times, as shown in range from 700 nm to 900 nm of Fig. 9. Detailed study how special films can be used to reduce IR component of the illumination spectrum is given in [23].

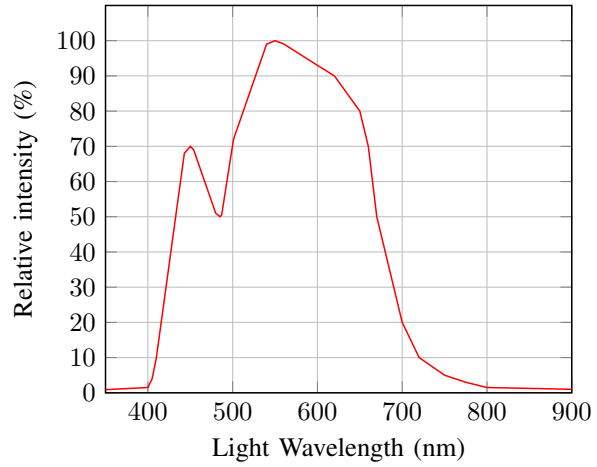

Fig. 9. Spectra of white LED surgical lamp.

IV. Virtual Zone Creation

We propose the creation of 3-D virtual geometrical structure by 3-D tracking tools on which fiducial markers are attached. The structure is created over the static scene. This approach eliminates problems like occlusion detection and how to fill the holes on the reconstructed surfaces, as is typically seen in 3-D reconstruction based on feature tracking, metric reconstruction, and object insertion [24].

A. 3-D Zone Creation

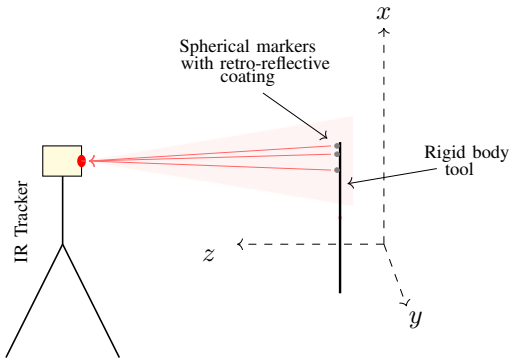

Fig. 10. Infrared flash and strong direct reflection.

Infrared Tracker sends flashlight to the geometrical structure with attached retro-reflective spheres as shown in Fig. 10. The main reflection from spheres defines their absolute position in the 3-D plane. A description of the number and determination of the location of spherical markers is generated during the tool characterization process in which the tool definition file is created. While tracking the rigid body, the IR camera returns the location of the geometric center of spheres. The position is calculated taking into account relative positions of each spherical marker to increase accuracy [11].

The position of tool tip, as shown in Fig. 11 can be calculated as a fixed offset from the rigid body origin. It is determined either by a block calibrator or pivoting procedure as described in [13].

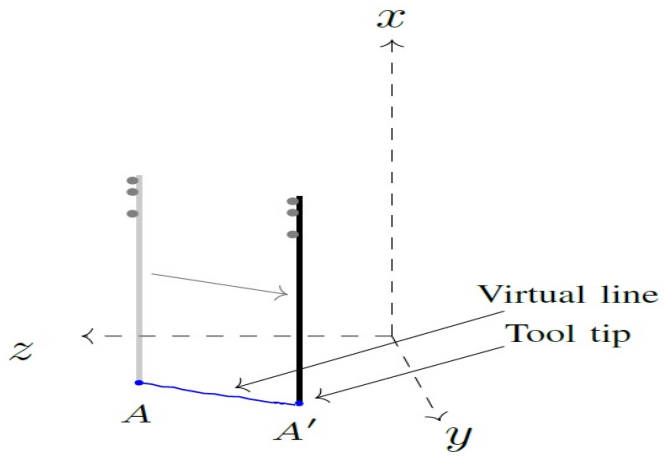

Fig. 11. Virtual line created by tool movement from A to A'.

When the tool moves form point A(x_1, y_1, z_1) to point A' (x_N, y_N, z_N), the camera reports the 3-D position of the tool tip points

$$(x_i, y_i, z_i) \quad i \in 1..N$$

The IR tracker reports 60 frames per second, so the tool tip can be used as a pencil to draw virtual lines like the one between point A and A' shown in Fig. 11.

In a similar way, we create the 3-D virtual conical structure. First, we point on the top of the structure, then to the bottom and after that drawing concentric circles go back to the upper part of the structure as shown in Fig. 12. In MIS surgery, the tip of the canonical structure is the trocar entry point, the bottom of the structure is the operation position, and the structure created by concentric circles is operation safe zone.

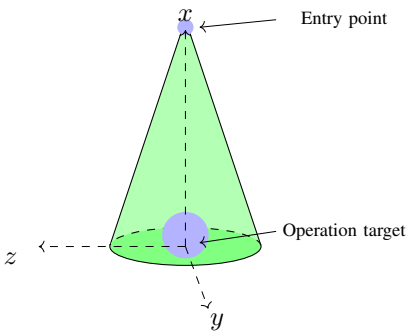

Fig. 12. Virtual 3-D zone.

B. Synthesis of Real Environments with Virtual Objects

Methods of virtual view generation can be classified into two categories: In the first, a full 3-D view of the scene is constructed and then reprojected to generate the virtual view. In the second method, virtual views are directly generated without having to estimate the scene structure [24].

Endoscopic camera position and orientation about a target object is determined by the position of the attached fiducial markers. We assume that the camera does not change its magnification. The virtual object should be inserted to target position according to camera position and orientation. When camera pose is changed, the position of virtual object 3-D zone must be changed too.

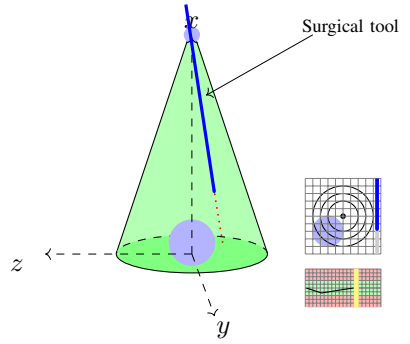

Fig. 13. Virtual 3-D zone with guidance data and distance to safe zone boundary indication.

Additional guidance of a tool to a target as shown in Fig. 13 is integrated. It handles the loss of depth perception related to the overlay of virtual models and endoscopic images [25].

The guidance provides information on a projected trajectory line, target and a depth bar that indicates the distance from the tip of the surgical tool, to the target.

Distance to the safe zone boundary shows in real-time the distance from the tip of the surgical tool to the safe zone edge.

A rigid tool with retro-reflective spheres can be attached to any laparoscopic surgical tool and used to show the position of the tooltip tracked during the operation. While the tool tip is inside the 3-D virtual safe zone, the operation is considered to be safe; when tool tip exits the virtual safe zone, an alarm warns the surgeon that the tool is not in the safe area.

This is different than existing systems of visual feature tracking [9], in which a process of intensive signal processing is used to indicate the position of tool tip inside the body. While both techniques are emerging, we believe that the method that embeds a virtual 3-D zone into the real-time stream is more promising because of ability to record surgical tools movements more accurately. That allows recording of a 3-D positions of any surgical instrument tip during the procedure. The record may be used to track possible inaccuracy in the process and to evaluate surgical skills quantitatively.

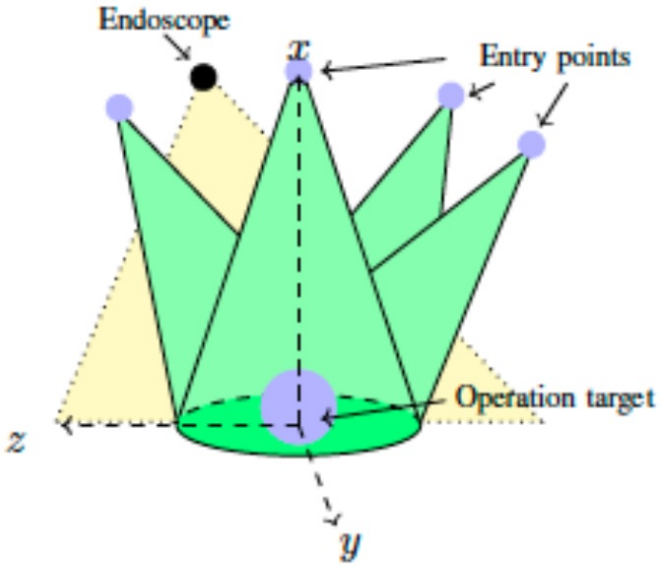

Fig. 14. Virtual 3-D multi-trocar zone.

It is possible to track up to five tools simultaneously. In Fig. 14 four entry points for surgical tools and one entry point for the endoscope is shown. The unique safe zone includes entry points of the tools and has a *crown* shape.

C. Endoscopic Image Overlay

Augmented reality visualization incorporates endoscopic images overlaid with virtual 3-D models. That technique is possible only if the camera is calibrated. The calibration creates a transition table between coordinate systems of the endoscope and the camera (${}^{endoscope}T_{camera}$) [25].

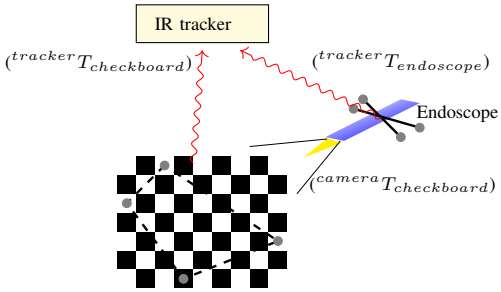

Fig. 15. Coordinate translation.

Transformations $({}^{tracker}T_{checkboard})$ and $({}^{tracker}T_{endoscope})$ are determined by reflections of IR signals from fiducial markers attached to the checkerboard and the endoscope. The translation $({}^{camera}T_{checkboard})$ is more complex; it needs intrinsic camera parameters and can be created by the method described in [25]. After the calibration that creates the transformation $({}^{endoscope}T_{camera})$ by tracking the endoscope, the IR tracker tracks the camera

$$({}^{track}T_{camera}) = ({}^{track}T_{endoscope}) \cdot ({}^{endoscope}T_{camera}) \quad (2)$$

Using this translation, we can insert 3-D safe zone like the one shown in Fig. 12 into the endoscopic view. Translation 2 is also used to show the position of surgical tool tips in the endoscopic view. Most of IR tracking systems can simultaneously track up to five tools. The accuracy of insertion of the 3-D virtual model in real-time view, according to clinical experiments reported in [25], has a mean value of 3.5 mm $\pm$ 1.9 mm.

D. Surface Tracking System

The system consists of a single GUI application, an endoscopic camera and the Polaris position tracking system (IR camera). The hardware components are used to track the position of a tool, either to define a boundary or determine the tool position. GUI components are supplied by the Qt [26] framework. Position tracking using an optical camera is handled by the OpenCV [27] framework. Position tracking using the Polaris system is handled by the Atamai Image Guided Surgery package (AIGS), which extends the Visualization Toolkit (VTK) [28] imaging library.

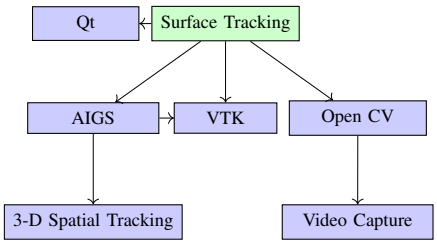

Fig. 16. System architecture.

The software system has many modules that include: *core logic*, *exit detection*, *tracking systems*, and *visualization*.

E. Physical Architecture

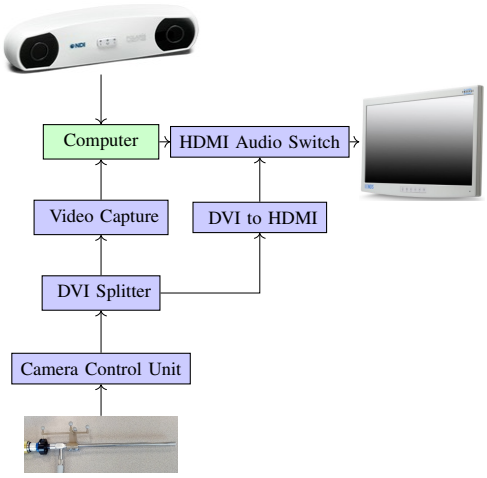

Fig. 17. Physical architecture.

Physical connection, as shown in Fig. 17, is designed such that in the event of a failure, the system will automatically switch to standard endoscopic view without safe zone. A failure in NDI tracking, or in the computer, will cause no harm. The switch to standard endoscopic view is instantaneous.

V. Telemedicine Robotics

Telemedicine robotics is an integral part of the telemedicine field, with the goal to provide specialized health care over a long distance.

Robotic systems make an impact in various areas of surgery including robotically assisted MIS.

All tele-robotic MIS systems are controlled by the surgeon from short-distance, like in the case of the Da Vinci Surgical System. For long distance, robotics tele-commands are passed through ethernet or by radio communication systems.

The technology that defines the safety boundary of robotic systems in the form of a 3-D virtual safety zone can be placed on the patient. Robotic tools controlled by a surgeon must always stay inside that safe zone. This is particularly important in systems where there is a delay. For instance what the surgeon sees is something that happens some time ago, equal to delay time. That means if a laparoscopic tool touches tissue outside of the safe zone, due to delay it will remain in a place where should not be for double the delay time. The safe zone can prevent such event by 1) advanced warning; and 2) automatic command that can stop robotic tools from exiting the safe zone, even if the surgeon gives such command to the robot.

A. Visual and Audio Warning

Real-time analysis of surgical tool movements may allow prediction of safe zone violation related to speed and direction. A visual and audio warning may be issued to the surgeon to make him aware that tool's movement may be harmful to the patient.

B. Automatic Control

In the case that a robotic surgical tool enters the unsafe zone, the system should activate auto-control and move surgical instruments back to safe zone. The condition in the form of the 3-D safe zone must never be breached. One of the promising areas of AR is telemedicine robotics. A safe zone, as a computer generated virtual object, has to be created before the operation starts. That zone is *invariant* meaning the condition must to be satisfied at all time during the operation.

C. Surgery in Space: the Future of Robotic Telesurgery

Handling body fluids and organs during open surgery in weightless environment could be very challenging. Thus, an endoscopic procedure that is performed in a confined body cavity presents a practical solution for surgery in weightlesness [29]. Proposed teleoperated systems for space surgery consists of a controller, slave robotic arms and sensory system feedback to the user. We believe a system that *alerts* the surgeon of a safe zone breach should always be present as the fourth component.

Some of the constraints related to telerobotic surgery in space are 1) the restriction on visual and tactile information by interposing robotics equipment; and 2) ground operator exhaustion due to remote control [5].

Constraints related to tactile information can be addressed by implementation of a system similar to the one presented in the project Robot in Medical Environment [30]. The system has a haptic master, and a 3-D infrared optical navigation device. However, this system does not establish the safe zone, or a virtual 3-D space in which all surgical instruments should be present during operation.

The control of tele-robotic systems is primarily based on image and video guidance [15]. Video guidance navigation associated bandwidth for the real-time image of resolution 640x480 is about 3.11Mbit/s. On the other hand, the navigation based on fiducial markers tracking needs only 56Kbps uplink, and 115Kbps downlink. The communication between International Space Station (ISS) and Ground is prone to disruption and delay. Communication to ISS exists in two bands:

- Ku-band 15GHz/43Mbps
- S-band 2GHz/ link up 72Kbps, down 192Kbps [5].

Video navigation can work only in Ku-band, while navigation based on fiducial markers tracking can work in both bands Ku-band and S-band.

Safe zone software may act as a low bandwidth redundancy for video failure or latency. By providing a coordinate system of robotic tools, the tracking software provides an additional security layer for ensuring the robotic surgical tool's error is limited. Virtual safe zone software can also act as a further resource optimization tool for video streaming. By relying upon information about coordinate systems, only the relevant parts of a picture are selected and translated back to Ground.

An expected future experiments in space is surgery on a live animal. The International Space Station (ISS) might be retired in 2024, but will be still open for unmanned and/or automated operation. Safety control of a remote dissection robot is one of the requirements of future medical experiments at ISS.

If NASA's proposed cis-lunar, and Martian exploration projects move forward, having the capability to perform surgery will be crucial - the crew will be to far away to turn back [31], [32].

VI. Predictive Projecting of Surgical Instruments Motion

To make IGS telesurgery feasible on the board of International Space Station, allowed delay should be up to 2s [33]. To accommodate this delay, predictive projecting of a tool's motion is presented on display. By adding constraints to predictive movements in the form of virtual safe zone, the surgeon on the Ground would be warned of possible damaging robotic movement ahead of time.

Artificial intelligence (AI) has many definitions, but the most comprehensive one is by Russel and Norvig who defined AI as *the study and design of intelligent agents, where an intelligent agent is a system that perceives its environment and takes actions that maximize its chances of success* [34].

Robotics surgery is one of the state of the art applications of AI. In a recent robotic surgery breakthrough [35], the Smart Tissue Autonomous Robot (STAR) stitched up the small intestines of a pig using its own vision, tools, and intelligence.

STAR performed at a higher level compared to trained surgeons who were given the same task. Intelligent robots capable of performing laparoscopic surgery, like SPORT Surgical Systems [36], are under development and are expected to be the commercial products in next few yeas.

SRI's tele-robotic surgical system, M7, expands the reach of surgical intervention by enhancing the precision of minimally invasive procedures and enabling surgeons to operate from afar [37]. The robot was tested in the NASA C-9 aircraft in simulated the microgravity of space. The goal is to create the procedure that may one day be used on the International Space Station, the Moon, or Mars.

We believe that for such critical procedures, like surgery in space, a system of warning should be in place. Such telerobotic surgical systems should be equipped with a system that will independently verify the position of surgical tools and issue a warning if the tools are not inside the safe zone. In addition to safety redundancy, getting the position of robotic arms by the independent system may be used for real-time robot behaviour analysis, and subsequently to increase situational awareness.

A. Post-procedure Analysis

It is possible to record the 3-D movement of each surgical tool and endoscope from the beginning to the end of the procedure. From the record, it is possible to quantitatively analyze the efficiency of the surgical procedure and discover possible areas of improvement. Recorded data of similar procedures performed by different surgeons can be used to compare surgeon effectiveness.

VII. Regulations

Medical devices are classified into Class I, II, and III and regulatory control increases from Class I to Class III [38]. We believe that most of these navigation technologies, including robotics, are Class II devices (moderate to high risk) to the FDA.

The augmented reality offers an additional feature; an option for the surgeon to disable it at any moment during a surgical procedure. A software watchdog controls the AR, so if there is any problem, the system automatically switches back to the non-augmented mode. Because of this, we believe the risk of AR usage is even lower than moderate, and can thereby speed up the regulatory approval process.

VIII. Conclusion

Development in computer vision and robotics are already changing the way in which surgery is being practiced [14]. AR in endosurgery is an emerging interdisciplinary field with potentially great impact on surgical procedures. The combination of pre-generated visual objects, real-time video streaming and real-time computer generated objects acquired by optical measurement systems in endosurgery is an example of a possible AR application in surgery. In addition to this, increasing computing power allows real-time image recognition that may provide additional information for the surgeon during the surgical procedure. The surgical tool tip movement inside the body can be recorded and quantitatively analyzed in the post-surgical process.

This procedure can increase the efficiency of laparoscopic surgery and estimate potential risks by calculating *smoothies* and speed of surgical tools during the procedure vs. distance to the safe zone boundary.

We believe that this system is also applicable in robotic assisted surgery: the position of the surgical tool held by the robotic arm can be verified in real-time by precise and accurate optical system. This technique may be especially useful in emerging field of space telesurgery.

Acknowledgment

The authors thank Mitch Wilson and Ashlin Kanawaty from Mariner Endosurgery Inc. for their help and comments.

References

[1] B. Furht, *Handbook of Augmented Reality*. Springer Publishing Company, Incorporated, 2011.

[2] F. P. Brooks, Jr., "The Computer Scientist As Toolsmith II," *Commun. ACM*, vol. 39, no. 3, pp. 61–68, Mar. 1996. [Online]. Available: http://doi.acm.org/10.1145/227234.227243

[3] T. Smith and B. M. Association, *The British Medical Association Complete Family Health Encyclopedia*. Dorling Kindersley, 1995. [Online]. Available: https://books.google.ca/books?id=6Y8QAAAACAAJ

[4] B. Nokovic, M. Wilson, and N. Nedialkov, "Laparoscopic Surgery System Calibrator and Method for Using the Same," 2016, Provisional patent US 62/439,845.

[5] JAXA, "Japan Aerospace Exploration Agency," 2017, http://global.jaxa.jp/.

[6] C. Bichlmeier, F. Wimmer, S. M. Heining, and N. Navab, "Contextual Anatomic Mimesis Hybrid In-Situ Visualization Method for Improving Multi-Sensory Depth Perception in Medical Augmented Reality," in *2007 6th IEEE and ACM International Symposium on Mixed and Augmented Reality*, Nov 2007, pp. 129–138.

[7] L. di Calcolo e Reti ad Alte Prestazioni del Consiglio Nazionale delle Ricerche, "Non Invasive Imaging For Advanced M.F.D." 2017, http://www.icar.cnr.it/en.

[8] H. Liao, *3D Medical Imaging and Augmented Reality for Image-Guided Surgery*. New York, NY: Springer New York, 2011, pp. 589–602. [Online]. Available: http://dx.doi.org/10.1007/978-1-4614-0064-6_27

[9] S. Payandeh, *Visual Tracking in Conventional Minimally Invasive Surgery*. Chapman and Hall/CRC, 2016.

[10] D. Bainbridge, D. L. Jones, G. M. Guiraudon, and T. M. Peters, "Ultrasound Image and Augmented Reality Guidance for Off-pump, Closed, Beating, Intracardiac Surgery," *Artificial Organs*, vol. 32, no. 11, pp. 840–845, 2008. [Online]. Available: http://dx.doi.org/10.1111/j.1525-1594.2008.00639.x

[11] *Accuracy assessment and interpretation for optical tracking systems*, vol. 5367, 2004. [Online]. Available: http://dx.doi.org/10.1117/12.536128

[12] NDI, "3D Measurement Tracking Technology," 2016, http://www.ndigital.com/.

[13] NDI, "Polaris tool digital design," 2007.

[14] W. Grimson, R. Kikinis, F. A. Jolesz, and P. Black, "Image-guided surgery," *Scientific American*, vol. 280, no. 6, pp. 54–61, 1999.

[15] S. Avgousti, E. G. Christoforou, A. S. Panayides, S. Voskarides, C. Novales, L. Nouaille, C. S. Pattichis, and P. Vieyres, "Medical Telerobotic Systems: Current Status and Future Trends," in *Biomedical engineering online*, 2016.

[16] B. Zitov and J. Flusser, "Image registration methods: a survey," *IMAGE AND VISION COMPUTING*, vol. 21, pp. 977–1000, 2003.

[17] R. Elfring, M. de la Fuente, and K. Radermacher, *Accuracy of Optical Localizers for Computer Aided Surgery*. Berlin, Heidelberg: Springer Berlin Heidelberg, 2009, pp. 328–330. [Online]. Available: http://dx.doi.org/10.1007/978-3-642-03906-5_90

[18] ISO, "Accuracy (trueness and precision) of measurement methods and results. Part 1: General principles and definitions," 1994.

[19] W. Beyer, *CRC Standard Mathematical Tables: 28th Ed.* CRC Press, 1987. [Online]. Available: https://books.google.ca/books?id=hEueMgEACAAJ

[20] A. D. Wiles, A. Likholyot, D. D. Frantz, and T. M. Peters, "A Statistical Model for Point-Based Target Registration Error With Anisotropic Fiducial Localizer Error." *IEEE Trans. Med. Imaging*, vol. 27, no. 3, pp. 378–390, 2008. [Online]. Available: http://dblp.uni-trier.de/db/journals/tmi/tmi27.html#WilesLFP08

[21] A. Danilchenko and J. M. Fitzpatrick, "General Approach to First-Order Error Prediction in Rigid Point Registration," *IEEE Transactions on Medical Imaging*, vol. 30, no. 3, pp. 679–693, March 2011.

[22] NDI, "Passive Polaris Spectra user guide - Revision 7," 2012.

[23] N. Zhu, S. Mondal, S. Gao, S. Achilefu, V. Gruev, and R. Liang, "Engineering light-emitting diode surgical light for near-infrared fluorescence image-guided surgical systems," *Journal of Biomedical Optics*, vol. 19, no. 7, p. 076018, 2014. [Online]. Available: http://dx.doi.org/10.1117/1.JBO.19.7.076018

[24] J.-S. Park, M. Y. Sung, and S.-R. Noh, *Virtual Object Placement in Video for Augmented Reality*. Berlin, Heidelberg: Springer Berlin Heidelberg, 2005, pp. 13–24.

[25] M. Fusaglia, K. Gavaghan, G. Beldi, F. Volonté, F. Pugin, M. Peterhans, N. Buchs, and S. Weber, *Endoscopic Image Overlay for the Targeting of Hidden Anatomy in Laparoscopic Visceral Surgery*. Berlin, Heidelberg: Springer Berlin Heidelberg, 2013, pp. 9–21. [Online]. Available: http://dx.doi.org/10.1007/978-3-642-38085-3_3

[26] T. Q. Company, "Cross-platform application framework," 2017, https://www.qt.io/.

[27] O. Foundation, "Open Source Computer Vision Library," 2017, http://opencv.org/.

[28] K. Inc., "The visualization toolkit," 2017, http://www.vtk.org/.

[29] T. Haidegger, J. Sándor, and Z. Benyó, "Surgery in space: the future of robotic telesurgery," *Surgical Endoscopy*, vol. 25, no. 3, pp. 681–690, 2011. [Online]. Available: http://dx.doi.org/10.1007/s00464-010-1243-3

[30] A. Rossi, A. Trevisani, and V. Zanotto, "A telerobotic haptic system for minimally invasive stereotactic neurosurgery," *The International Journal of Medical Robotics and Computer Assisted Surgery*, vol. 1, no. 2, pp. 64–75, 2005. [Online]. Available: http://dx.doi.org/10.1002/rcs.17

[31] Spacenews, "Nasa moving ahead with plans for cis-lunar human outpost," 2017, http://spacenews.com/nasa-moving-ahead-with-plans-for-cislunar-human-outpost/.

[32] NASA, "Prepare for the human exploration of mars," 2017, https://mars.nasa.gov/programmissions/science/goal4/.

[33] I. Mendez, R. Hill, D. Clarke, G. Kolyvas, and S. Walling, "Robotic Long-distance Telementoring in Neurosurgery," *Neurosurgery*, vol. 56, pp. 434–440, 2005.

[34] S. J. Russell and P. Norvig, *Artificial Intelligence: A Modern Approach*, 2nd ed. Pearson Education, 2003.

[35] E. Strickland, "Autonomous Robot Surgeon Bests Humans in World First," 2017, http://spectrum.ieee.org.

[36] T. Medical, "SPORT Surgical System," 2017, http://www.titanmedicalinc.com/.

[37] S. International, "M7 Surgical Robot," 2017, https://www.sri.com/.

[38] FDA, "Classification of medical devices," 2017, https://www.fda.gov/.